UPPSALA
UNIVERSITET

Digital Comprehensive Summaries of Uppsala Dissertations from the Faculty of Science and Technology **666**

Light-Metal Hydrides for Hydrogen Storage

MARTIN SAHLBERG

ACTA
UNIVERSITATIS
UPSALIENSIS
UPPSALA
2009

ISSN 1651-6214
ISBN 978-91-554-7585-7
urn:nbn:se:uu:diva-107380

Dissertation presented at Uppsala University to be publicly examined in Häggsalen, Ångströmlaboratoriet, Lägerhyddsvägen 1, Uppsala, Friday, September 25, 2009 at 10:15 for the degree of Doctor of Philosophy. The examination will be conducted in English.

Abstract
Sahlberg, M. 2009. Light-Metal Hydrides for Hydrogen Storage. Acta Universitatis Upsaliensis. *Digital Comprehensive Summaries of Uppsala Dissertations from the Faculty of Science and Technology* 666. 56 pp. Uppsala. 978-91-554-7585-7.

Demands for zero greenhouse-gas emission vehicles have sharpened with today's increased focus on global warming. Hydrogen storage is a key technology for the implementation of hydrogen powered vehicles. Metal hydrides can claim higher energy densities than alternative hydrogen storage materials, but a remaining challenge is to find a metal hydride which satisfies all current demands on practical usability. Several metals store large amounts of hydrogen by forming a metal hydride, e.g., Mg, Ti and Al. The main problems are the weight of the material and the reaction energy between the metal and hydrogen.

Magnesium has a high storage capacity (7.6 wt.% hydrogen) in forming MgH_2; this is a slow reaction, but can be accelerated either by minimizing the diffusion length within the hydride or by changing the diffusion properties. Light-metal hydrides have been studied in this thesis with the goal of finding new hydrogen storage compounds and of gaining a better understanding of the parameters which determine their storage properties. Various magnesium-containing compounds have been investigated. These systems represent different ways to address the problems which arise in exploiting magnesium based materials. The compounds were synthesized in sealed tantalum tubes, and investigated by *in situ* synchrotron radiation X-ray powder diffraction, neutron powder diffraction, isothermal measurements, thermal desorption spectroscopy and electron microscopy.

It is demonstrated that hydrogen storage properties can be improved by alloying magnesium with yttrium or scandium. Mg-Y-compounds decompose in hydrogen to form MgH_2 nanostructures. Hydrogen desorption kinetics are improved compared to pure MgH_2. The influence of adding a third element, gallium or zinc has also been studied; it is shown that gallium improves hydrogen desorption from YH_2. $ScAl_{1-x}Mg_x$ is presented here for the first time as a hydrogen storage material. It absorbs hydrogen by forming ScH_2 and Al(Mg) in a fully reversible reaction. It is shown that the hydrogen desorption temperature of ScH_2 is reduced by more than 400 °C by alloying with aluminium and magnesium.

Keywords: Metal-hydrogen compounds, hydrides, hydrogen storage, X-ray diffraction, neutron diffraction, thermal desorption spectroscopy

Martin Sahlberg, Inorganic Chemistry, Department of Materials Chemistry, Box 538, Uppsala University, SE-75121 Uppsala, Sweden

ISSN 1651-6214
ISBN 978-91-554-7585-7
urn:nbn:se:uu:diva-107380 (http://urn.kb.se/resolve?urn=urn:nbn:se:uu:diva-107380)

Publications included in this thesis

This thesis is a summary of the following publications, referred to in the text by their Roman numerals:

I Hydrogen desorption studies of the $Mg_{24}Y_5$-H system: Formation of Mg tubes, kinetics and cycling effects
C. Zlotea, M. Sahlberg, S. Oezbilen, P. Moretto and Y. Andersson.
Acta Materialia, 56 (2008) 2421-2428

II Hydrogen absorption in Ti doped $Mg_{24}Y_5$
C. Zlotea, M. Sahlberg, P. Moretto and Y. Andersson
Journal of Alloys and Compounds, *In submission*

III YMgGa
M. Sahlberg, T. Gustafsson and Y. Andersson
Acta Crystallographica, E63 (2007) i195

IV YMgGa as a hydrogen storage compound
M. Sahlberg, C. Zlotea, P. Moretto and Y. Andersson
Journal of Solid State Chemistry, 182 (2009) 1833-1837

V Hydrogen absorption in Mg-Y-Zn ternary compounds
M. Sahlberg and Y. Andersson
Journal of Alloys and Compounds, 446-447 (2007) 134-137

VI Sc_2MgGa_2 and Y_2MgGa_2
M. Sahlberg and Y. Andersson
Acta Crystallographica, C65 (2009) i7-i8

VII A new material for hydrogen storage, $ScAl_{0.8}Mg_{0.2}$
M. Sahlberg, P. Beran, T. Kollin Nielsen, Y. Cerenius, K. Kadas, M.P.J. Punkkinen, L. Vitos, O. Eriksson, T.R. Jensen and Y. Andersson
Accepted for publication in Journal of Solid State Chemistry

VIII Fully reversible hydrogen absorption and desorption reactions with $Sc(Al_{1-x}Mg_x)$, x = 0.0, 0.15, 0.20
M. Sahlberg, C. Zlotea, M. Latroche and Y. Andersson
In manuscript

Reprints were made with permission from the publishers.

My contributions to paper I-VIII

I	Synthesis of the samples, XRD, part of writing.
II	Synthesis of the samples, XRD, part of writing.
III	Major part of the experimental work and the writing.
IV	Major part of the experimental work, part of PCT and TDS, first author.
V	Major part of the experimental work and the writing.
VI	Major part of the experimental work and the writing.
VII	Major part of the experimental work, first author.
VIII	Major part of the experimental work and the writing.

Contents

Abbreviations

DFT	Density functional theory
DTA	Differential thermal analysis
EDS	Energy dispersive X-ray spectroscopy
EMTO	Exact muffin-tin orbitals
GGA	Generalized gradient approximation
HDDR	Hydrogenation-disproportionation-desorption-recombination
NPD	Neutron powder diffraction
SEM	Scanning electron microscopy
SR-XRD	Synchrotron radiation X-ray powder diffraction
TEM	Transmission electron microscopy
TDS	Thermal desorption spectroscopy
TG	Thermal gravimetry
TM	Transition metal
TPD	Temperature programmed desorption
UHV	Ultra-high vacuum
XRD	X-ray diffraction

1. Introduction

The greenhouse effect has been a major political issue during the last years. There has also been a global effort to reduce the emission of carbon dioxide in the atmosphere, even though there is still a very long way to go. These issues have led to an increasing interest for clean energy systems and vehicles with no emission of greenhouse gases[1,2].

For the zero emission vehicle idea to be realized a new way to store energy must be used. There are two main groups of zero-emission energy carriers that are being considered for automotive applications, batteries and hydrogen[2].

Batteries have the advantage that you only need an electric outlet in order to "refuel" your vehicle. However, the amount of energy that can be stored in today's batteries is limited, leading to a practical limit of the driving range of the vehicle. The battery charging time is also too long, usually more than 4 hours.

When hydrogen reacts with oxygen, water is formed and energy is released, as described below. The released energy can be used to power a vehicle with water as the rest product. There are two ways to use the energy in hydrogen: by burning the hydrogen and get the energy as heat or by reactions with oxygen in a fuel cell, to form electricity. There are two key advantages with using a hydrogen powered fuel cell vehicle instead of a normal gasoline powered vehicle: the total "well-to-wheels" energy efficiency increases by a factor of three[3] and there is no emission of greenhouse gases.

$$H_2 + \tfrac{1}{2}O_2 \rightarrow H_2O + \text{energy}$$

There are many different ways to produce hydrogen[4]. Renewable energy can be used to produce hydrogen, such as photovoltaic hydrogen generation that include light generated electricity and water splitting[5]. Another way is to use microorganisms like green algae that produce hydrogen under anaerobic conditions[6]. However, most hydrogen produced today comes from reforming natural gas, oil or coal[3]. The chemical energy per mass in hydrogen, 142 MJ/kg, is very high compared to today's fuels. A completely clean energy system is achieved if renewable energy is used to produce hydrogen gas, as described in Figure 1.1.

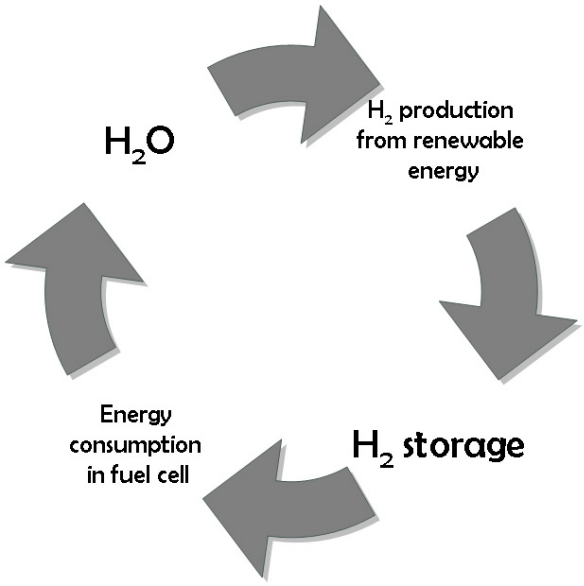

Figure 1.1. The hydrogen energy cycle.

Hydrogen powered vehicles usually have a longer driving range than electric vehicles but suffer in the sense of storing the hydrogen gas in an efficient and convenient way. There are three major ways to store hydrogen, as shown in Figure 1.2. Pressurized gas and cryogenic liquid are two conventional ways to store hydrogen, well working but not good enough for a permanent solution. One problem with both systems is the energy density; none of the systems fulfils the demands set on the system size and weight[2,7]. Metal-hydrogen compounds are alloys or complexes that react with hydrogen and form compounds, they are generally good in energy density but have other severe limitations for practical usability, such as a high required hydrogen pressure and slow reactions.

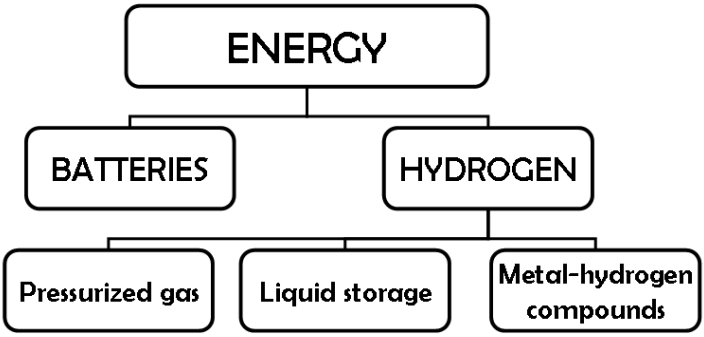

Figure 1.2. Family tree of two different ways to store energy for vehicular applications.

In order to execute the transition to hydrogen as an energy carrier several demands on the storage must be fulfilled. First of all, the hydrogen storage system must be safe. Secondly, the storage system must fulfil a number of demands concerning storage ability, practical use, lifetime and cost[2]. The European Commissions High Level Group for Hydrogen and Fuel Cells Technologies states in "Hydrogen Energy and Fuel Cells – A vision of our future" that the European Union in 2050 should have a Hydrogen-oriented economy and estimates that 35% of all new cars will be fuelled by zero carbon hydrogen in 2040[1]. The U.S. Department of Energy believes that the transition to hydrogen-powered fuel cell vehicles will occur within the next 10-15 years (2006)[2].

2. The scope of this thesis

In this thesis, the metal-hydrogen interaction is investigated, with focus on phase analysis and hydrogen absorption and desorption properties. The goals are to find new hydrogen absorbing alloys and to better understand how the crystal structure and the chemical composition affect the storage properties. Some of the investigated compounds decompose during hydrogen absorption; but the results still give important knowledge of how different materials interact with hydrogen. The influence of chemical composition, crystal structure and particle size are discussed.

The search for new hydrogen absorbing alloys is important as none of the materials that we know today fulfil all the material demands that are set for onboard hydrogen storage[7]. In this thesis, compounds formed by elements with different hydrogen interaction properties have been synthesized. One or two elements that form stable hydrides (yttrium, magnesium and/or scandium) are combined with elements that do not as easily interact with hydrogen (zinc, gallium and aluminium) but might increase the hydrogen dissociation and diffusion. These phase diagrams are only partly known and there are most probably new hydrogen absorbing compounds, which could have improved absorption and desorption properties, suitable for vehicular applications.

To get a better understanding of the parameters influencing the absorption and desorption properties several different methods have been used such as time resolved *in-situ* synchrotron radiation X-ray powder diffraction, neutron powder diffraction, electron microscopy and thermo gravimetric methods. By combining these methods it was possible to study the different reactions occurring during hydrogen loading and unloading and to use this information to design new materials with desired properties.

3. Metal hydrides as hydrogen storage materials

The use of metal hydrides as hydrogen storage materials is an old idea that was brought to life again with increasing interest in using hydrogen as an energy carrier. In 1866, Thomas Graham published a paper on hydrogen absorption in palladium[8], where he stated that 1 vol. palladium can store 643.3 vols. hydrogen. This was the first time that the ability of metals to absorb hydrogen was published. It took however another century until the classical $LaNi_5$ hydrogen storage alloys were discovered[9,10]. Today, these types of compounds (AB_5) are widely used in rechargeable Ni-MH batteries.

There are many different compounds that can accommodate hydrogen. The different types of hydrides were classified in a more detailed description by Gary Sandrock[11]. In this description, he differentiated between the alloy hydrides and the complex hydrides, as seen in Figure 3.1. Complexes are mixed covalent-ionic compounds, that typically have a larger hydrogen capacity than alloys, but generally have a higher temperature of hydrogen desorption and are not as easily reversible. The alloy hydrides are metals or alloys that absorb hydrogen and form stable hydrides. They are usually prepared by combining a metal that forms stable binary hydrides and one that catalyses the dissociation of the H_2-molecule e.g. titanium and iron.

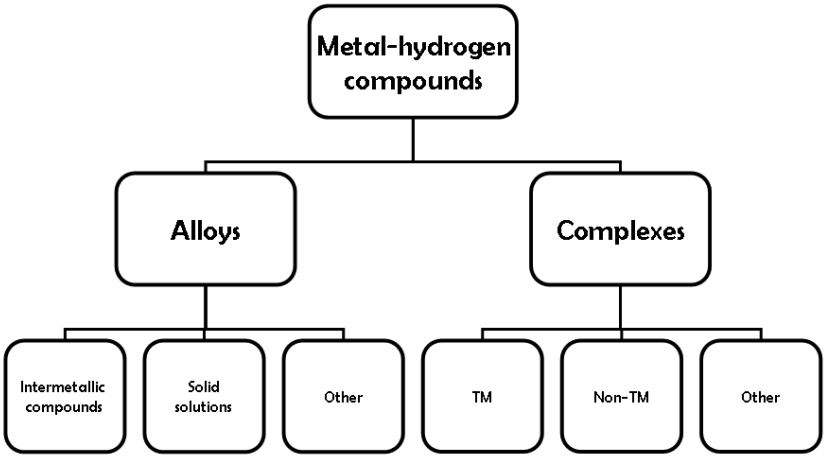

Figure 3.1. Family tree of metal hydrides, as described by Sandrock[11].

3.1 Complexes

When certain transition metals (TM) are combined with a group I or II element in hydrogen gas a $[TM\text{-}H_x]^{y-}$ anionic complex is formed with the group I or II elements as corresponding cations e.g. Mg_2NiH_4[12,13]. These types of hydrides are called chemical or complex hydrides. Complex hydrides also exist for non-TM metals such as aluminium in e.g. sodium alanate ($NaAlH_4$). $NaAlH_4$ is a compound that has gained significant international interest as a potential hydrogen storage compound after it was proven to store hydrogen reversibly when catalysed with titanium chloride[14,15]. There are however several problems with these types of hydrides except problems with reversibility, Bogdanović *et al.* claims in their recent review on complex hydrides[16] that:

> "Therefore, realistically, even $NaAlH_4$, which is presently the most promising candidate material, will not meet all the criteria necessary to provide a practical means of hydrogen storage."

3.2 Alloys

As stated above, one alloy system that is commonly used today is the $LaNi_5$-based alloys. This is one of the few metal hydride systems that fulfil all demands on material stability etc. set by industry for practical use. Unfortunately, the hydrogen storage capacity in $LaNi_5$ is only 1.49 wt.% which revoke any plans to use the material for vehicular applications.

The use of magnesium based alloys as hydrogen storage compounds has been studied for a long time[17,18 19,20]. Magnesium dihydride contains several times more hydrogen per unit weight than the classical AB_5-type hydrides, the maximum capacity is 7.6 wt%. However, there are several problems with magnesium dihydride as a storage material. The first and most limiting problem is that the kinetics of hydrogen absorption is very slow, even at high temperatures. The kinetics of hydrogen absorption can be greatly improved by alloying magnesium with other metals, e.g. Cu[21]. Mg_2Cu absorbs hydrogen while decomposing to MgH_2 and $MgCu_2$. Even with an excess of magnesium the presence of Mg_2Cu catalyses the reaction between magnesium and hydrogen and improves the kinetics.

Hydrogen absorption in an alloy is commonly described as a two-step process, as seen in Figure 3.2. The metal initially dissolves a small amount of hydrogen in the metal matrix, forming a solid solution α-phase. As the hydrogen content increases the interaction between hydrogen and metal atoms become more important and a hydride β-phase is formed. If the hydrogen absorption is performed at equilibrium conditions these two phases co-

exist until the whole material has turned into the hydride β-phase. This reaction is reversible.

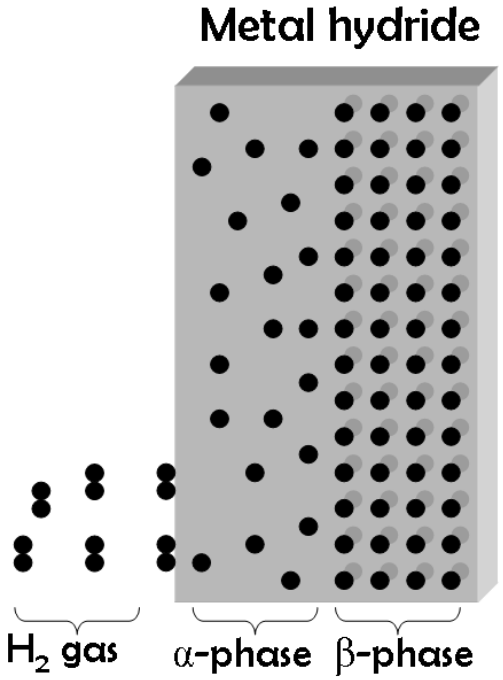

Figure 3.2. Schematic image of hydrogen in a metal. The solid solution α-phase and the hydride β-phase.

3.2.1 Alloys with yttrium and magnesium

Buchner *et al.* have investigated Mg-$Mg_{17}Y_{13}$ alloys with respect to vehicular applications[22]. They found that adding a small amount of $Mg_{17}Y_{13}$ to the Mg matrix improved the kinetic properties significantly.

Solid solutions of Y in Mg were studied by Douglass, where he found that small amounts of yttrium or yttrium and nickel significantly improved the kinetics of hydrogen desorption[23]. The possibility of yttrium to improve the kinetics in magnesium was later studied by Chacon *et al.* where they showed that adding a small amount of yttrium in a thin film of magnesium enhanced the hydrogen diffusion through the film[24]. There has also been reports by Goto *et al.* of a ternary magnesium-yttrium-hydride, MgY_2H_6, synthesized at very high pressures (5 GPa) [25]. However, from desorption measurements it was evident that not all hydrogen could be recovered. Only 1.4 wt% could be stored reversibly.

3.2.2 Alloys with scandium and magnesium

The hydrogen desorption properties of solid solutions of scandium in magnesium was studied by Ogawa *et al.* where they showed that with 10% scandium in magnesium the amount of desorbed hydrogen was only about two thirds of the expected amount from the formula (Mg-Sc)H_2. They argued that the low desorption depended on a very strong bond between scandium and hydrogen[26].

Deuterium absorption in the intermetallic compound $Mg_{0.65}Sc_{0.35}$ was studied by Latroche *et al.* This compound absorbed deuterium and a phase transition from a pseudo CsCl-type structure to a CaF_2-type structure occurred[27,28]. However, it was not possible to remove all deuterium from this compound and the reaction was only partly reversible.

The different alloys investigated in this thesis are listed in Table 1, together with their space-group and type structure.

Table 1. *Crystal structures of the investigated alloys*

Compound	**Space-group**	**Type structure**
$Mg_{24}Y_5$	$I\bar{4}3m$	α-Mn
YMgGa	$P\bar{6}2m$	ZrNiAl
$Mg_{12}YZn$	-	-
$Mg_3Y_2Zn_3$	$Fm\bar{3}m$	$AlMnCu_2$
Sc_2MgGa_2	$P\frac{4}{m}bm$	Mo_2FeB_2
$Sc(Al_{1-x}Mg_x)$	$Pm\bar{3}m$	CsCl

4. Experimental

4.1 Material synthesis

All samples were prepared using direct reactions between the elements. Since magnesium is a highly volatile and reactive element at high temperatures common synthesis methods cannot be used to prepare the required samples. To avoid the problems with magnesium the synthesis was performed inside a sealed tantalum tube. Tantalum is a highly stable metal that can sustain high temperatures without reacting with other metals.

Figure 4.1. Upper part from the left: Pieces of aluminium, scandium and magnesium. Lower part: A sealed tantalum tube.

Appropriate amounts of the elements were placed in a tantalum tube that was welded shut inside an argon filled glovebox. The sealed tube was placed

in an induction furnace (Figure 4.2) and heated to the desired temperature. No reaction between the sample and the tantalum tube was observed for any of the samples.

Figure 4.2. Synthesis in the induction furnace.

The tube was opened inside an argon filled glovebox to avoid oxygen contamination of the samples. Some of the samples had to be grounded and subsequently heat treated in order to obtain homogeneous materials. The heat treatments were performed in evacuated silica ampoules.

4.2 Hydrogen absorption

4.2.1 High pressure synthesis

The high pressure furnace used the solid-gas interaction model for hydrogen absorption in the mother compounds. The grounded sample was placed in a stainless steel tube, that was evacuated down to ~1 Pa and flushed several times with hydrogen (100 kPa) to remove oxygen and water from the system. The short exposure time to air when loading the reactor is considered to

be negligible. The sample was hydrogenated at temperatures from 20 to 500 °C.

By monitoring the hydrogen pressure as a function of temperature the absorption temperature was investigated. The total amount of absorbed hydrogen was determined by the gravimetric method i.e. weighting the sample before and after hydrogenation.

4.2.2 Deuterium absorption

For samples investigated with neutron diffraction, the alloys were reacted with deuterium. All absorption reactions were performed in the same way as for hydrogen.

4.3 Diffraction

Diffraction is a phenomenon that occurs when waves or wavelike matter (X-rays, electrons or neutrons) interacts with crystalline matter. Diffraction is coherent scattering with constructive and destructive interference that occurs at discrete directions.

4.3.1 X-ray powder and single crystal diffraction

X-rays are scattered by the electrons surrounding the nucleus of the atoms in the crystal. The scattering factor for each atom is to a first approximation directly proportional to the number of electrons surrounding the nucleus i.e. the atomic number. The contributions from the hydrogen atoms in the X-ray diffraction (XRD) patterns are therefore very small compared to the heavier metal atoms, and are therefore difficult to locate in the crystal structure. It is also a problem to differentiate between two adjacent elements in the periodic table.

In paper I - IV & VI - VIII, XRD measurements were performed using a Bruker D8 diffractometer with a Våntec position-sensitive-detector (PSD, 4° opening) with CuKα_1-radiation. In paper V a Guinier-Hägg-type focusing camera with CuKα_1-radiation was used for phase analysis and the X-ray powder diffraction profiles were collected on a high resolution Stoe & Cie Gmbh STDI transmission X-ray powder diffractometer with a small linear position-sensitive-detector (PSD, 6° opening) with CuKα_1-radiation.

Single crystal data used for the structure determinations of YMgGa and Sc_2MgGa_2 were recorded on a Bruker APEX diffractometer equipped with a 2KCCD detector. The single crystals were mounted on thin glass fibres.

4.3.2 Synchrotron radiation X-ray powder diffraction

In situ synchrotron radiation X-ray powder diffraction (SR-XRD) measurements were performed at the MAX-II Synchrotron in Lund, Sweden, using the Beamline I711[29]. The wavelength used was refined to 1.09994 Å and the X-ray exposure time was 30 s/scan. The diffracted intensities were measured using a Mar165 CCD detector. A sapphire single crystal tube was used as a sample holder and a gas supply system allowing changes in both gas and pressure via a vacuum pump was attached to the sample cell, see Figure 4.3. The sample cell was heated by resistive heating (tungsten wire) and the temperature was measured by a thermocouple placed inside the sapphire tube. This setup allowed changes of pressure and temperature during the measurements.

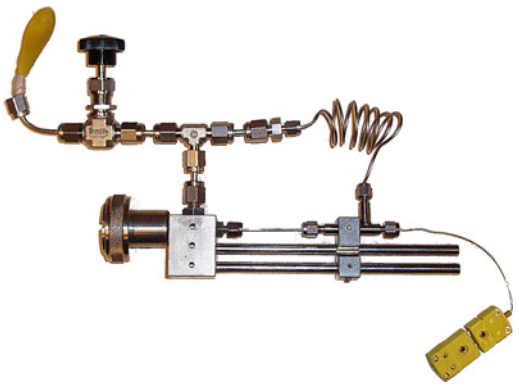

Figure 4.3. Sample holder used for SR-XRD.

4.3.3 Neutron powder diffraction

In contrast to X-rays, neutrons are diffracted by the nucleus of the atoms in a quantum-mechanical process. Neutron powder diffraction (NPD) is a very useful tool to investigate hydrides since the scattering length of the isotopes of hydrogen, protium (^{1}H) and deuterium (^{2}H) are comparable with the heavier elements. However, neutron diffraction of protium causes incoherent scattering, and deuterated samples are used in the crystal structure determinations.

The NPD data presented in this thesis was recorded at the LVR15 reactor in Rez near Prague, using instrument HOKAN6. The sample was contained in a vanadium cylinder. The neutron beam was monochromatized to 1.274 Å by three bended Si(422) single crystals. Diffractograms between 5-120° in 2Θ were recorded in steps of 0.1°. The measurements were performed at room temperature.

4.3.4 Crystal structure determination and refinement

Single crystal diffraction intensities were collected using the program SMART and unit cell refinements were performed using the program SAINT[30]. The crystal structures were solved and refined using the program SHELX[31].

Crystal structure refinements from powder XRD and NPD were performed using the Rietveld method[32] implemented in the program FULLPROF[33].

4.4 Absorption / desorption isotherms and thermal desorption spectroscopy

A very powerful tool to investigate the reactions during hydrogen absorption and desorption is to study the reaction isotherms. As stated in section 3.2, hydrogen absorption in metals commonly starts with a solid solution of hydrogen in the metal, and when the maximum solid solution is reached a hydride phase starts to form. When the hydrogen-saturated metal coexists with the hydride phase, Gibbs' phase rule requires the equilibrium pressure to be constant at any given temperature below the critical temperature[34], see Figure 4.4. The length of the plateau determines the amount of hydrogen that can be accommodated reversibly with only a small pressure variation.

The enthalpy and entropy changes during hydrogen absorption and desorption is calculated from the equilibrium pressure at different temperatures. The relation between the equilibrium pressure (P) and temperature (T) is given by the Van't Hoff equation:

$$\ln(P/P_0) = \Delta H/(RT) - \Delta S/R$$

where P_0 is atmospheric pressure, ΔH and ΔS are the changes in enthalpy and entropy, respectively, and R is the gas constant. For almost all hydrides, the hydrogen absorption reaction is exothermic ($\Delta H < 0$).

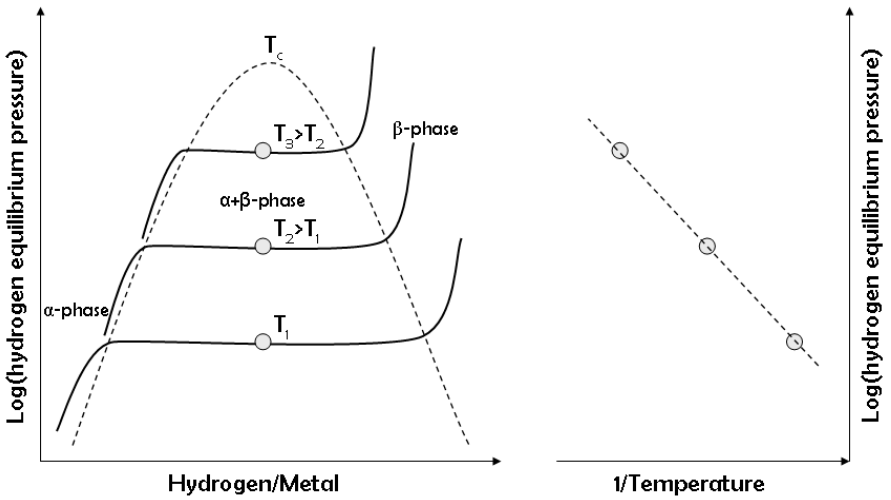

Figure 4.4. Schematic image of a pressure-composition-temperature plot and a Van't Hoff plot.

The thermodynamic properties obtained from isothermal measurements gives information on the driving force for the transformations, but it cannot give information on how fast the reaction will proceed. To get information on the kinetics of a reaction a different method must be used. For a reaction to take place there is usually an activation barrier that must be overcome before the reaction starts, i.e. the activation energy. By performing Kissinger analysis[35], the activation energy for a reaction can be obtained. In the area of hydrogen storage materials this method is known as thermal desorption spectroscopy (TDS) or temperature programmed desorption (TPD). This method is commonly used to determine the activation energy for hydrogen release from a material.

By heating the metal hydride at a constant heating rate and recording the hydrogen pressure, a thermal desorption spectrum is obtained. The activation energy can be calculated from TDS spectra recorded at different heating rates using the Kissinger equation:

$$d\ln(\beta/T_{max}^2)/d(1/T_{max}) = -E_A/R$$

where β is the applied heating rate, T_{max} is the temperature of maximum desorption rate i.e. the maximum hydrogen pressure, E_A is the activation energy and R is the gas constant. By calibrating the system using a hydride with a known hydrogen content this method is commonly used for quantitative determination of the hydrogen content in a material[36].

The pressure-composition-temperature (PCT) analysis and thermal desorption spectroscopy used in Paper I, II and IV were performed in a volu-

metric instrument (Hiden Isochema) designed for measurements of hydrogen absorption / desorption isotherms and total amount of thermally desorbed hydrogen. TDS measurements in Paper IIIV were performed using an ultra-high vacuum (UHV) furnace equipped with a dynamic sampling mass spectrometer.

4.5 Microstructural analysis

Scanning electron microscopy (SEM) is a technique to look at materials in very high magnification. By scanning a material with an electron beam and detecting the secondary- and backscattered electrons an image of the material is constructed. Another phenomenon occurring when the electron beam interacts with the sample is the generation of X-rays with an element specific energy. By detecting these X-rays one can perform elemental analysis, energy dispersive X-ray spectroscopy (EDS).

The SEM images presented in this thesis were recorded using a LEO 400 microscope, a LEO 1550 microscope or a high resolution LEO Supra 50 microscope. Elemental analysis was made in a LEO 440 scanning electron microscope with an EDAX EDS spectrometer. The samples were either grounded and placed on a carbon film or polished. Quantitative analyses were performed with the ZAF correction method.

Transmission electron microscopy (TEM) is another method to study materials in very high magnification. However, in TEM one can also perform electron diffraction and get information on the crystal structure of the investigated sample. The TEM analysis was performed using a FEI-TECNAI F-20 instrument operating at 200 kV.

4.6 Thermal analysis

Differential thermal analysis (DTA) and thermal gravimetry (TG) are two methods that are used to study the changes in energy and mass during a chemical reaction. The mass and temperature of the sample is measured as the sample is heated at a constant rate, and the mass change and exothermal/endothermal properties of the reaction is obtained.

DTA/TG measurements in Paper V were performed using a NETZSCH, STA 409 PC thermal analysis instrument. The samples were measured under flowing argon atmosphere. The measurements were made with increasing temperature from 25 to 500 °C, using a heating rate of 20 °C/min.

4.7 Density functional theory calculations

Density functional theory (DFT) [37] has been widely used for calculations in physics and chemistry. DFT has been very successful in both predicting and explaining many material properties observed from experiments. Studies of hydrogen in metals can be greatly improved by gaining information on the electronic band structure and making it possible to compare the total energy of different hydride structures.

The *ab initio* calculations presented in this thesis are based on DFT formulated within the generalized gradient approximation (GGA) [38] for the exchange-correlation functional applying the Exact Muffin-tin Orbitals method (EMTO). For a more detailed description of the calculations and discussion of the theoretical results, see the theory part of Paper VII and references therein.

5. Y-Mg-based alloys

5.1 $Mg_{24}Y_5$

The intermetallic compound $Mg_{24}Y_5$ crystallizes in the cubic space group $I\bar{4}3m$, a variant of the α-Mn-type structure[39]. The homogeneity of the phase extends from 84 to 87 at.% magnesium at 525 °C[40]. The unit cell parameter was determined to 11.2507(2) Å at the magnesium-rich boundary of the $Mg_{24+x}Y_5$ phase.

Hydrogen absorption in $Mg_{24}Y_5$ has been investigated thoroughly in our group[41]. It has been shown that hydrogen absorption occurs by decomposition of $Mg_{24}Y_5$ into MgH_2 and YH_3. During hydrogen absorption long (>150 μm) one-dimensional single crystal whiskers of MgH_2 with thicknesses from 100 nm were formed. The formation of these types of microstructures during hydrogen absorption is a desired property since hydrogen diffusion through magnesium hydride is very slow. Thus, by forming whiskers the hydrogen diffusion length inside magnesium is minimized which should improve the kinetics of hydrogen loading and unloading. Hydrogen desorption from hydrogenated $Mg_{24}Y_5$ was studied in Paper I.

Desorption from the hydrogenated $Mg_{24}Y_5$, a mixture of MgH_2 and YH_3, was a two-reaction process forming pure Mg and YH_2. The complete desorption of yttrium dihydride did not occur at the investigated temperatures (<400 °C) [42]. Hydrogen desorption from the MgH_2 whiskers and microparticles produced magnesium tubes and carved particles. Figure 5.1 shows a SEM image of the $Mg_{24}Y_5$ sample after desorption. The walls of the magnesium tubes were very thin, in the range of nanometres. By investigating the desorbed sample with TEM it was evident that the tubes consisted of single crystalline magnesium.

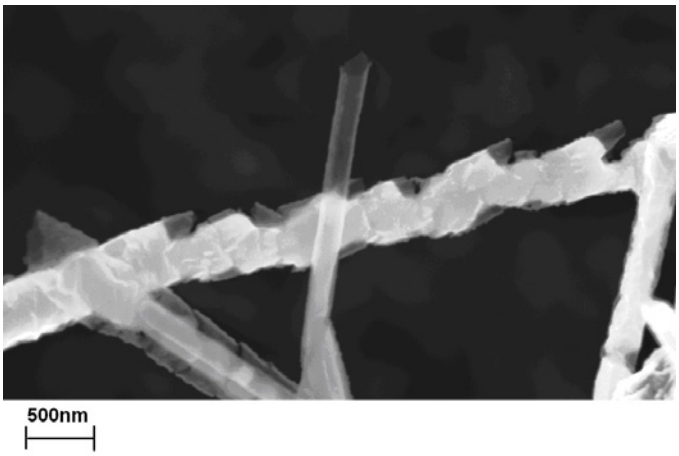

Figure 5.1. SEM image of desorbed $Mg_{24}Y_5$-H showing carved magnesium tubes.

By performing TDS on the hydrogenated $Mg_{24}Y_5$ and comparing with commercial MgH_2 it was proven that the kinetics of hydrogen desorption improved when alloying with yttrium. The temperature of maximum desorption rate (T_m) is 30 °C lower for $Mg_{24}Y_5$-H as compared with MgH_2. By performing Kissinger analysis it was also observed that the activation energy for hydrogen desorption (E_a) was lower for $Mg_{24}Y_5$-H than for MgH_2, 153(10) kJ/mol and 182(10) kJ/mol respectively.

The morphological changes of the whiskers during hydrogen loading/unloading cycling were studied by SEM after 5, 16 and 36 cycles. During the first cycles the whiskers kept their microstructure, but with many fractures in the whiskers. Further cycling of the material destroyed the unidirectional shape and the whiskers were transformed into clusters of nanoparticles, thus lowering the grain size even further.

By monitoring the storage capacity and T_m during cycling it was observed that T_m was decreased with cycling, proving that the kinetics were improved. This was in good agreement with the SEM investigations as the grain size was also lowered during cycling. It was also seen that the storage capacity was lowered with cycling. The lowering in total storage capacity was attributed to partial oxidation of magnesium during cycling. The presence of small amounts of oxygen could not be avoided in the experimental setup. The partial oxidation of magnesium was also observed from XRD, showing small amounts of MgO with cycling.

5.1.1 $Mg_{24}Y_5$-Ti

Doping of $Mg_{24}Y_5$ with 0.5 at.% titanium was investigated in Paper II to evaluate if the hydrogen storage properties could be improved by a catalyst.

Titanium has been commonly used as a catalyst material for sodium alanate and has been proven to catalyze the reversibility in that compound[15].

From SEM-EDS investigations of the alloy it was shown that titanium did not react with the other elements during synthesis, small titanium particles were randomly dispersed in the sample. The sample consisted mainly of the $Mg_{24+x}Y_5$-phase with only small amounts of Mg and Ti. The small amounts of titanium were not possible to detect in the XRD profile as seen in Figure 5.2.

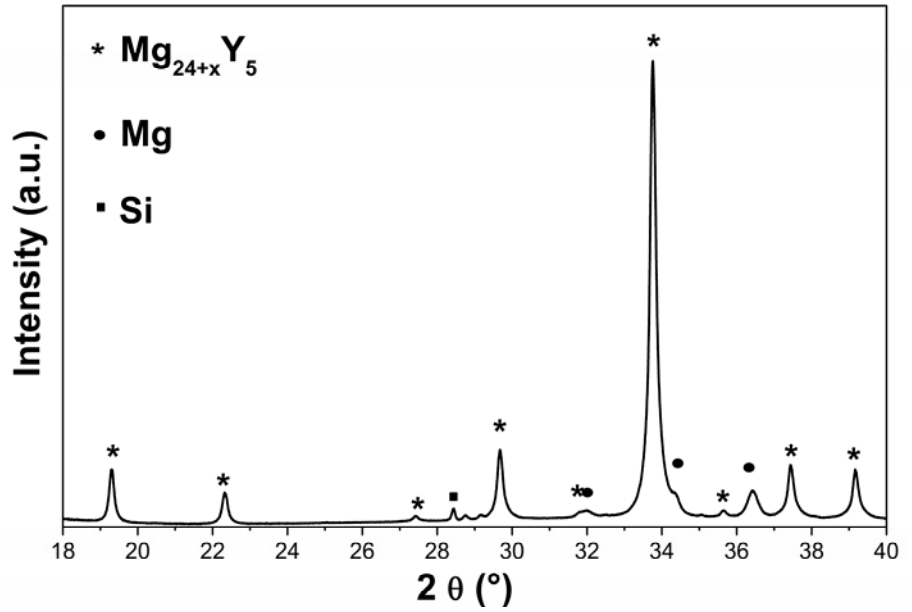

Figure 5.2. XRD pattern of the Mg-Y-Ti alloy. Si was used as internal calibration standard.

Hydrogen absorption and desorption formed MgH_2 whiskers and carved Mg tubes respectively, the same behaviour as for pure $Mg_{24}Y_5$. PCT measurements showed that the maximum reversible storage capacity for the alloy was 4.8 wt.% at 375 °C. Several PCT curves were measured between 345 °C and 385°C. The enthalpy of hydrogen desorption (ΔH) was calculated using the Van't Hoff equation, see Figure 5.3. The calculated ΔH = -68 kJ/molH_2 was in good agreement with previously reported values for MgH_2[17].

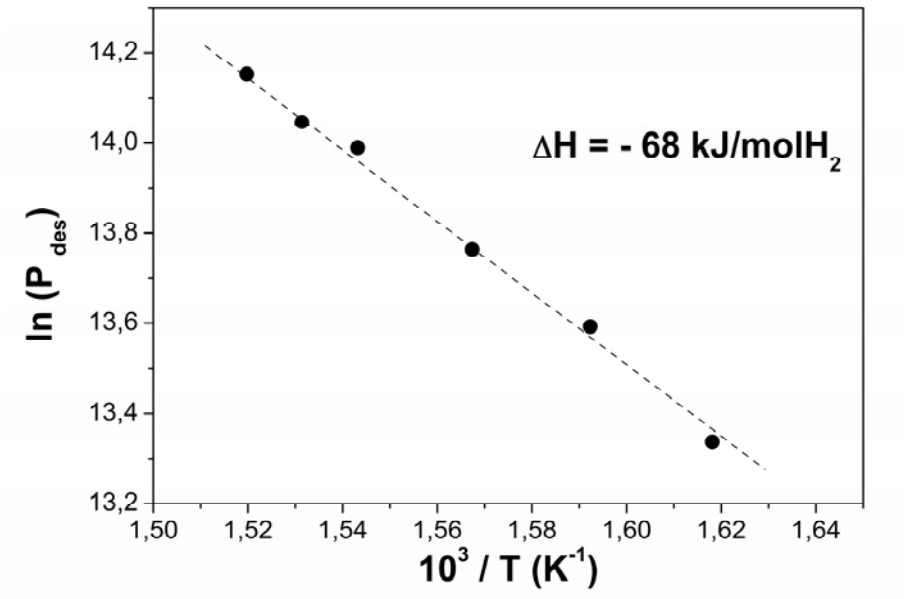

Figure 5.3. Van't Hoff plot of the hydrogen desorption from the hydrogenated Mg-Y-Ti alloy.

The kinetic properties of hydrogen desorption were studied by TDS. The activation energy of desorption (E_a) was determined using the Kissinger method. The obtained value E_a = 150(10) kJ/mol, was in good agreement with earlier studies of pure $Mg_{24}Y_5$. Thus, there were no indications of thermodynamic or kinetic improvements due to the presence of titanium particles dispersed in the alloy.

5.2 YMgGa

The previous results on Mg-Y[24,41] and Mg-Ga[43] showed a potential of improving the storage properties of magnesium by alloying with yttrium and gallium. A ternary YMgGa-phase was reported earlier by Kraft *et al.* [44] to be hexagonal with the unit cell axes a = 7.268(4) Å and c = 4.413(2) Å.

Large (several mm) single crystals of the ternary compound were synthesized and the crystal structure was determined using X-ray single crystal diffraction intensities. As seen in Paper III, the crystal structure was proven to be the hexagonal ZrNiAl-type structure[45], which is an ordered version of the Fe_2P-type structure[46]. The atomic arrangement along the c-axis is shown in Figure 5.4. The structure can be described as a network of magnesium and gallium atoms, with yttrium situated inside distorted hexagonal channels.

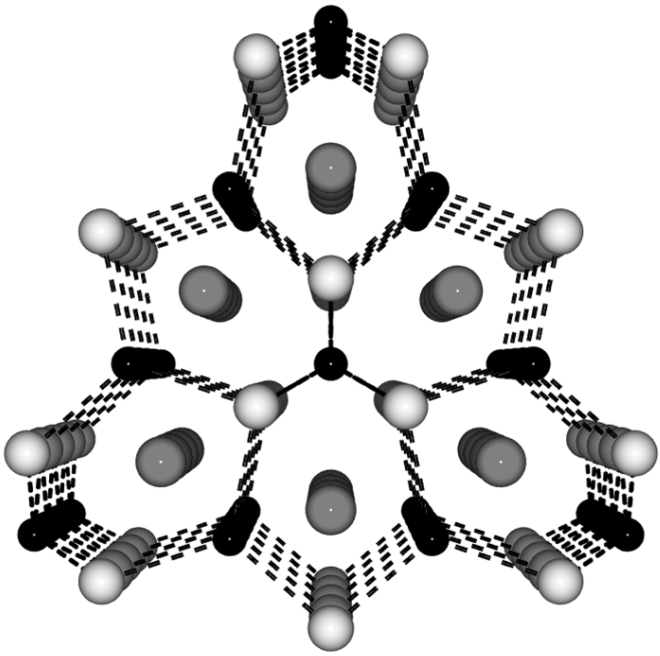

Figure 5.4. YMgGa structure along the c-axis. Mg, Ga and Y are light gray, black and dark gray respectively.

The hydrogen storage properties of YMgGa were studied in Paper IV. The mother compound was grounded to a powder and investigated with XRD, shown in Figure 5.5. Small amounts of Y_2MgGa_2 and YGa were observed but the amounts were estimated to be less than 10%.

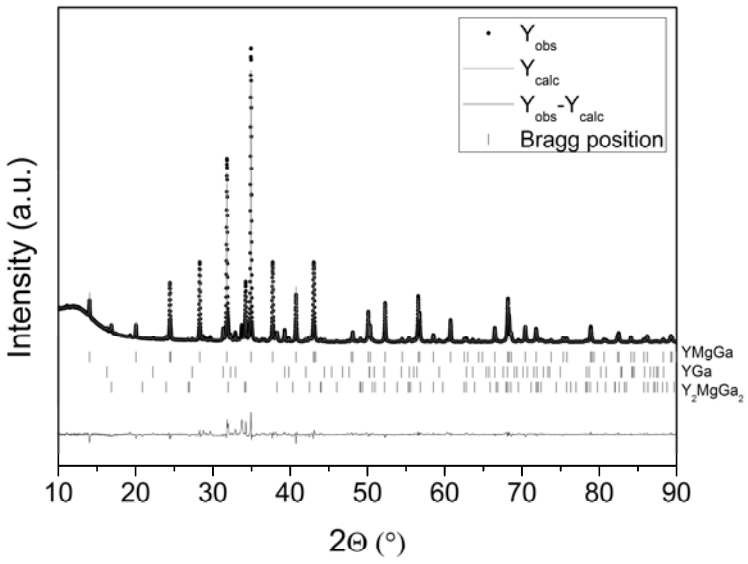

Figure 5.5. XRD pattern of the mother compound YMgGa.

The mother compound absorbed hydrogen while decomposing to YH_3 and MgGa. The reaction was complete for hydrogen pressures above 6 MPa at 375 °C, see Figure 5.6. Small amounts of Mg_2Ga, YGa_2 and MgH_2 were also formed.

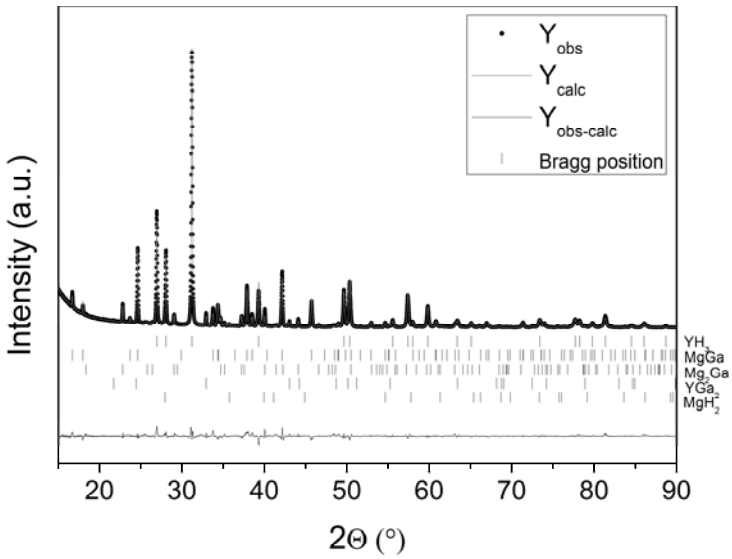

Figure 5.6. XRD pattern of YMgGa, hydrogenated at 6 MPa and 375 °C.

Isothermal measurements at 375 °C showed, that ~2.1 wt% hydrogen was absorbed during the first hydrogenation as seen in Figure 5.7. The reaction was only partially reversible, about half of the hydrogen was desorbed. In the second isotherm was this amount, ~1.1 wt%, absorbed. Another isotherm was measured after 13 hydrogen absorption/desorption cycles. The shape of this isotherm was very similar to the second isotherm showing that the material was stable during cycling.

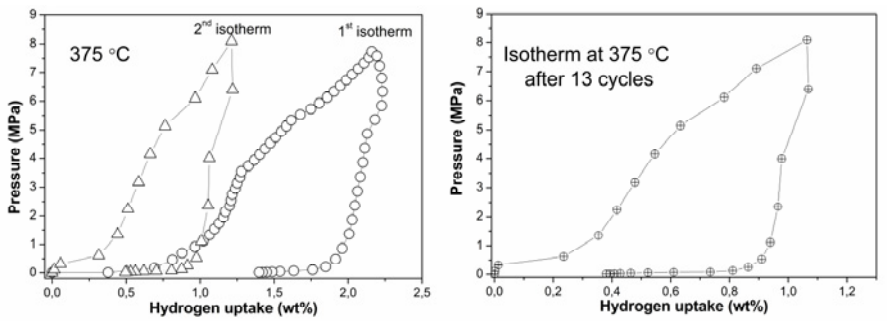

Figure 5.7. PCT of YMgGa, measured at 375 °C. Left: first and second isotherm. Right: Isotherm after 13 cycles.

TDS was performed, up to 450 °C, on the fully hydrogenated sample and the corresponding XRD pattern of the desorbed sample is shown in Figure 5.8.

During desorption there was formation of YH_2, YGa_2, Mg and YMgGa. The amount of YH_2 in the desorbed sample was significantly less than the amount of YH_3 in the hydrogenated sample. This suggests that there was hydrogen desorption from YH_2 which was unexpected since pure YH_2 is reported not to desorb hydrogen below 800 °C[42]. The destabilisation of YH_2 was explained by the formation of YGa_2. The standard enthalpies of formation of YH_2 and YGa_2 have previously been determined to -227 kJ/mol[47] and -193 kJ/mol[48] respectively. These values are quite similar which can explain the formation of YGa_2 during hydrogen desorption. It is interesting to notice the reformation of YMgGa during desorption.

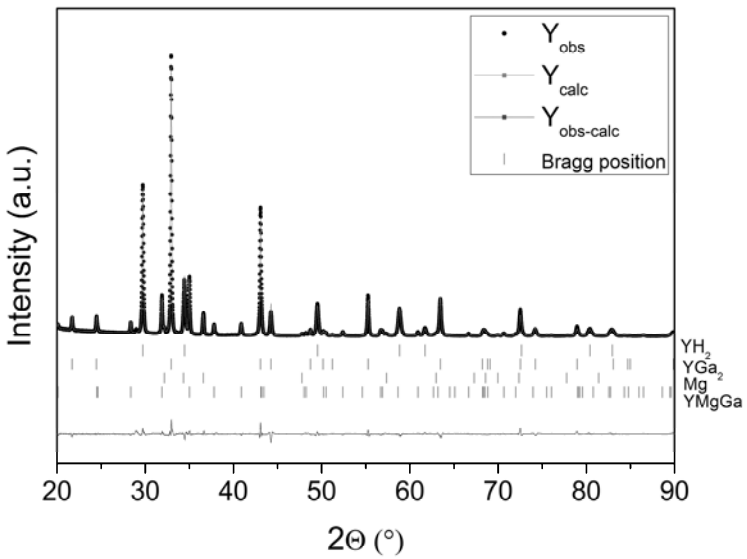

Figure 5.8. XRD pattern of desorbed YMgGa.

TDS was performed on the cycled sample. It was observed that the onset temperature for hydrogen desorption was lowered from 320 to 260 °C, furthermore T_m was lowered from 379 to 363 °C. Cycling was not affecting the thermodynamic properties, as seen from PCT. However, it improved the kinetics of hydrogen desorption by lowering the onset temperature and T_m.

5.3 $Mg_3Y_2Zn_3$

The ternary Mg-Y-Zn compounds, $Mg_{12}YZn$ and $Mg_3Y_2Zn_3$ were investigated from a hydrogen storage point of view in Paper V. It was found that

for both mother compositions, $Mg_3Y_2Zn_3$ was the dominating phase, suggesting that $Mg_3Y_2Zn_3$ is the most stable phase in the magnesium rich corner of the ternary diagram. It was also observed that $Mg_{12}YZn$ decomposed above 300 °C to Mg and $Mg_3Y_2Zn_3$. Since there was no hydrogen absorption below 400 °C $Mg_{12}YZn$ was excluded from further investigations.

$Mg_3Y_2Zn_3$ crystallizes in the cubic $AlMnCu_2$-type structure, space group $Fm\bar{3}m$. The unit cell parameter was determined to 6.9116(6) Å. $Mg_3Y_2Zn_3$ absorbed hydrogen by decomposing into MgH_2, YH_3 and $MgZn_2$. This reaction occurred for hydrogen pressures above 1 MPa and a temperature of 400 °C. The hydrogen desorption properties were partially studied by DTA/TG, at temperatures up to 500 °C, see Figure 5.9. An endothermal peak was observed at ~430 °C together with a decrease in mass. Mg_3YZn_6 and YH_2 were formed as judged from XRD patterns. Therefore, it was concluded that the yttrium dihydride was destabilized by magnesium and zinc. A similar behaviour was observed in the YMgGa-H system.

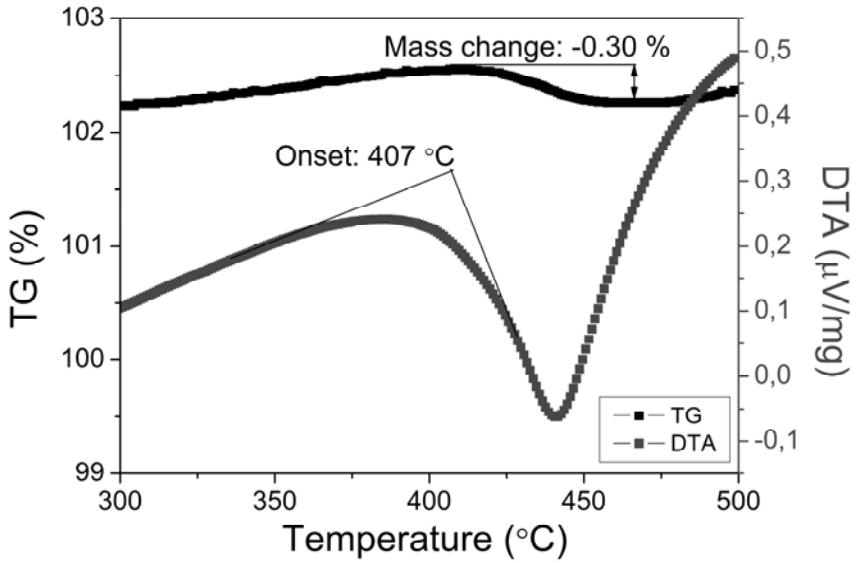

Figure 5.9. DTA/TG on hydrogenated $Mg_3Y_2Zn_3$.

5.4 Summary of the Y-Mg-based alloys

The results from Paper I-V show that all the studied Y-Mg-based alloys decomposed during hydrogen absorption. This is due to the very strong bond between yttrium and hydrogen with the high standard enthalpy of formation

for YH_2 of -227 kJ/mol[47]. For the binary yttrium-magnesium compound one-dimensional single crystal whiskers of MgH_2 were formed during hydrogen absorption. Upon desorption the solid whiskers transformed to carved tubes of magnesium. However, there was no desorption observed from YH_2 and thus the desorption products were yttrium dihydride and metallic magnesium. The kinetics of hydrogen desorption was increased both by alloying and by cycling the material.

Introducing a third element to the Mg-Y system made it possible to destabilize the yttrium dihydride and release hydrogen at temperatures far below the reported values for pure YH_2. For YMgGa, it was even possible to partially reform the mother compound. By alloying yttrium and magnesium with gallium it was possible to both gain a partially reversible system and increase the kinetics of hydrogen desorption. This opens up the possibility to tailor the storage properties of alloy materials for hydrogen storage.

6. Sc-Mg-based alloys

6.1 Sc_2MgGa_2

The crystal structures of Sc_2MgGa_2 and Y_2MgGa_2 were studied in Paper VI. Large single crystals of Sc_2MgGa_2 were synthesized and the crystal structure was determined using single crystal diffraction intensities. Sc_2MgGa_2, and isostructural Y_2MgGa_2, crystallizes in the tetragonal Mo_2FeB_2-type structure[49].The ternary Mo_2FeB_2-type structure is an ordered version of the binary U_3Si_2-type structure[50], where the two uranium sites are occupied by different atoms. A SEM image of the well crystallized sample is shown in Figure 6.1.

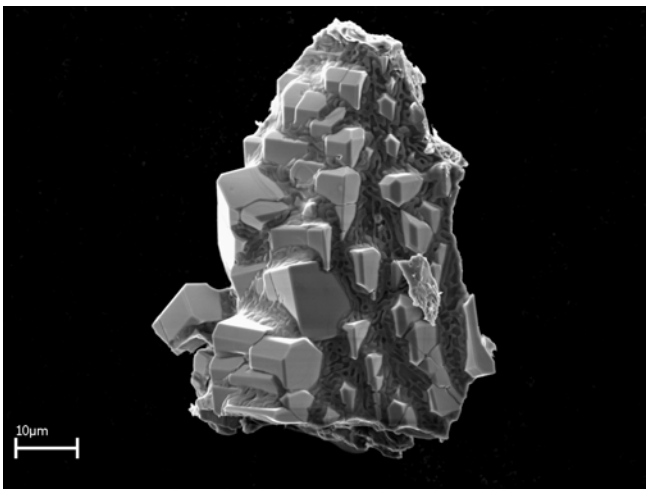

Figure 6.1. SEM image of a sample with the overall composition $ScMg_4Ga$. Crystals of Sc_2MgGa_2 are shown in the matrix.

The Sc_2MgGa_2 structure can be described as two intergrown slabs of CsCl and AlB_2, this is emphasized in Figure 6.2. The compositions in the slabs are ScMg and $ScGa_2$, respectively. In the z-direction the structure is layered with one layer of magnesium and gallium atoms at z = 0 and another layer of scandium atoms at z = 0.5. All three crystallographically unique atoms oc-

cupy special positions with the site symmetries *m2m* and *4/m* for (Sc, Ga) and Mg, respectively.

Attempts were made to hydrogenate the compound but in the investigated temperature and pressure range (up to 450 °C and 5MPa) there was no hydrogen absorption.

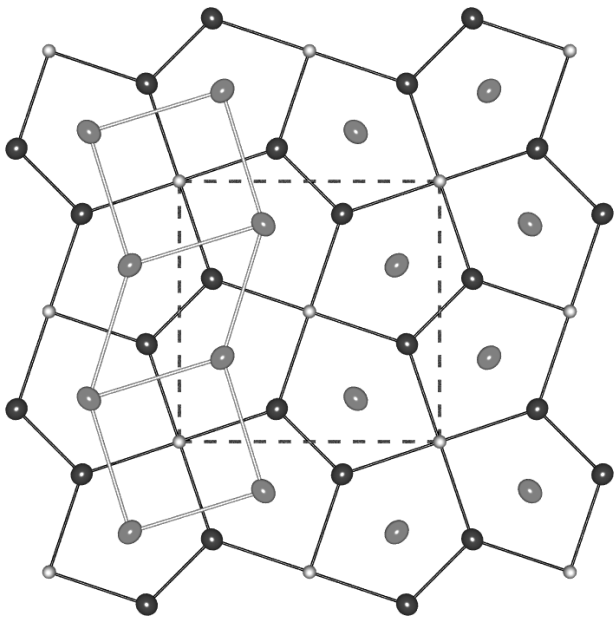

Figure 6.2. The crystal structure of Sc_2MgGa_2, along the c-axis. Sc, Mg and Ga atoms are grey, white and black respectively.

6.2 $Sc(Al_{1-x}Mg_x)$, $x \leq 0.2$

6.2.1 $ScAl_{0.8}Mg_{0.2}$

Hydrogen absorption in $ScAl_{0.8}Mg_{0.2}$ was studied in Paper VII. The mother compound was synthesized and the crystal structure was determined to be the cubic CsCl-type structure, with scandium in the 1a site (0, 0, 0) and aluminium and magnesium in the 1b site (0.5, 0.5, 0.5). This was in agreement with previous investigations of the ternary Al-Mg-Sc system[51]. The unit cell parameter was refined to 3.4106(1) Å. The structure refinement showed only a small mixing of the atoms with 90(1)% Sc and 10(1)% Al/Mg on the 1a

site and 87(1)% Al/Mg and 13(1)% Sc on the 1b site. A XRD pattern of the mother compound is shown in Figure 6.3.

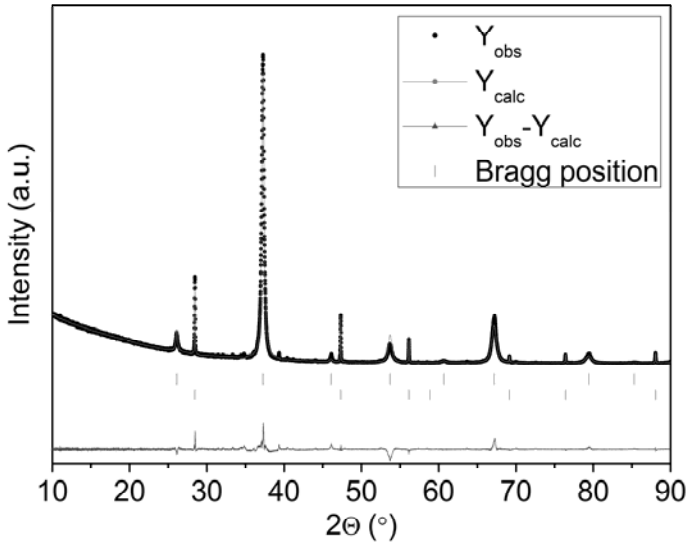

Figure 6.3 XRD pattern of $ScAl_{0.8}Mg_{0.2}$. The lower phase is silicon, used as an internal calibration standard.

The sample was hydrogenated *in situ* at a hydrogen pressure of 10 MPa and a temperature increase from 20 to 400 °C at a heating rate of 10 °C/min. After ramping, the temperature was kept at 400 °C for the rest of the experiment. In Figure 6.4, it is shown that the hydrogen absorption started just below 400 °C and the compound decomposed to ScH_2 and Al(Mg). After hydrogen absorption the pressure was released to vacuum. At the investigated temperature the hydrogenated sample was stable under vacuum.

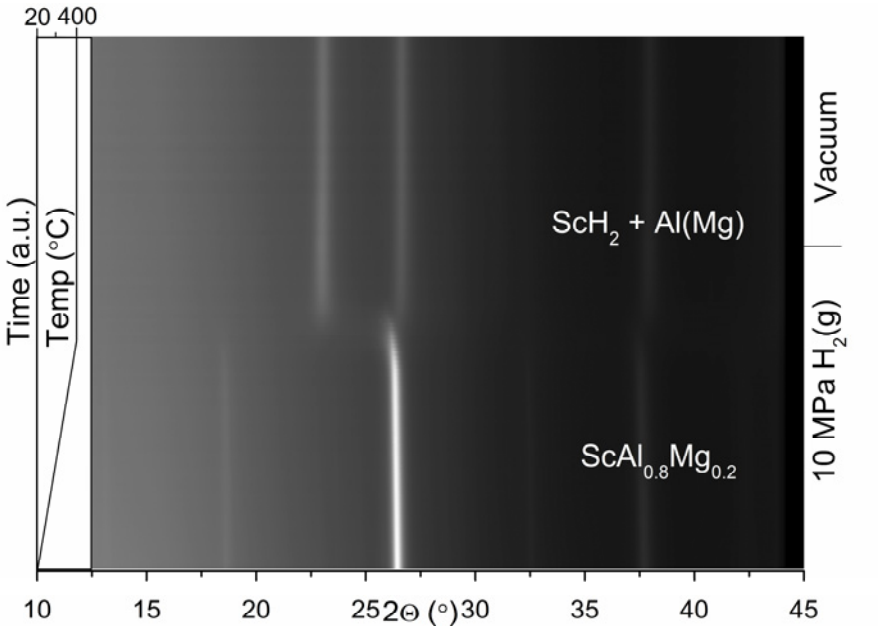

Figure 6.4. Hydrogen absorption in $ScAl_{0.8}Mg_{0.2}$ investigated with *in situ* SR-XRD.

In Figure 6.5, the decomposition from $ScAl_{0.8}Mg_{0.2}$ to ScH_2 and Al(Mg) is emphasized. The hydrogen absorption was very rapid; the total time for the decomposition was ~3 min.

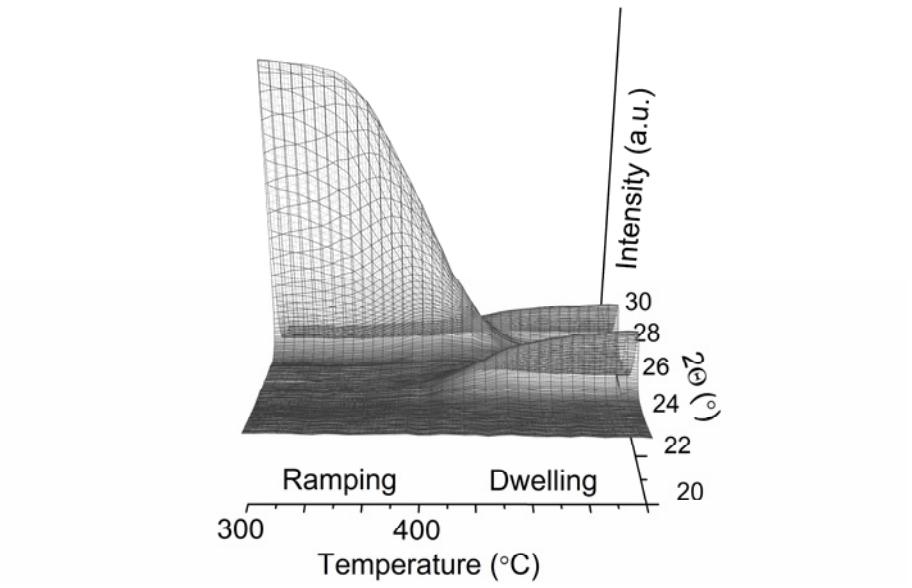

Figure 6.5. *In situ* SR-XRD data showing the decomposition from $ScAl_{0.8}Mg_{0.2}$ to ScH_2 and Al(Mg).

The sample was deuterated and investigated with NPD (Figure 6.6) to confirm the crystal structure. The refinement showed that the deuterated phase was indeed ScD_2 which has the cubic CaF_2-type structure. The refinement also showed that the deuterium site (0.25, 0.25, 0.25) was fully occupied giving the final composition ScD_2. This result was in agreement with the gravimetric measurements.

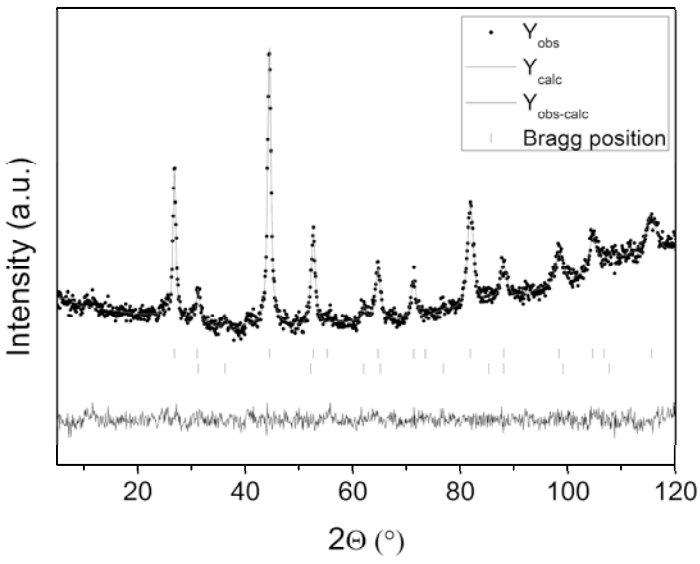

Figure 6.6. NPD pattern of deuterated $ScAl_{0.8}Mg_{0.2}$. The upper and lower tics marks the Bragg positions of ScD_2 and Al(Mg) respectively.

TDS was performed to evaluate the desorption properties. A linear temperature increase was applied under vacuum and the partial hydrogen pressure was measured with a dynamic sampling mass spectrometer. The sample started to desorb hydrogen at 300 °C and two desorption peaks were observed, as shown in Figure 6.7.

By performing Kissinger analysis the activation energy of hydrogen desorption was calculated. The activation energy for the small and large peaks was 139 kJ/mol and 185 kJ/mol, respectively.

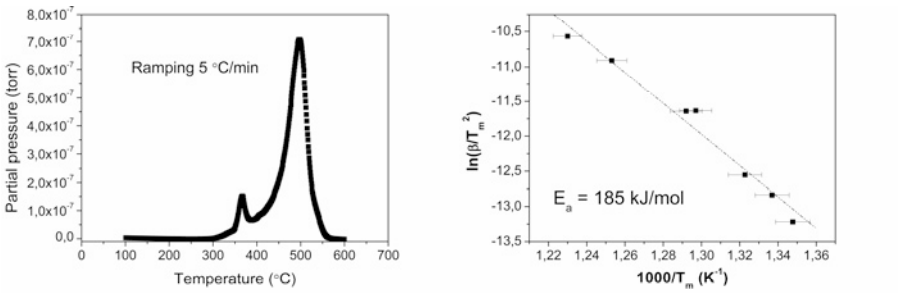

Figure 6.7. Left: TDS pattern of hydrogenated $ScAl_{0.8}Mg_{0.2}$. Right: Kissinger plot of hydrogenated $ScAl_{0.8}Mg_{0.2}$. The error bars indicate an estimated error of ± 5 °C.

From XRD it is evident that the hydrogen storage in $ScAl_{0.8}Mg_{0.2}$ is fully reversible, as seen in figure 6.8. The compound adopts the hydrogenation-disproportionation-desorption-recombination (HDDR) behaviour[52] commonly used in the production of Nd-Fe-B permanent magnets.

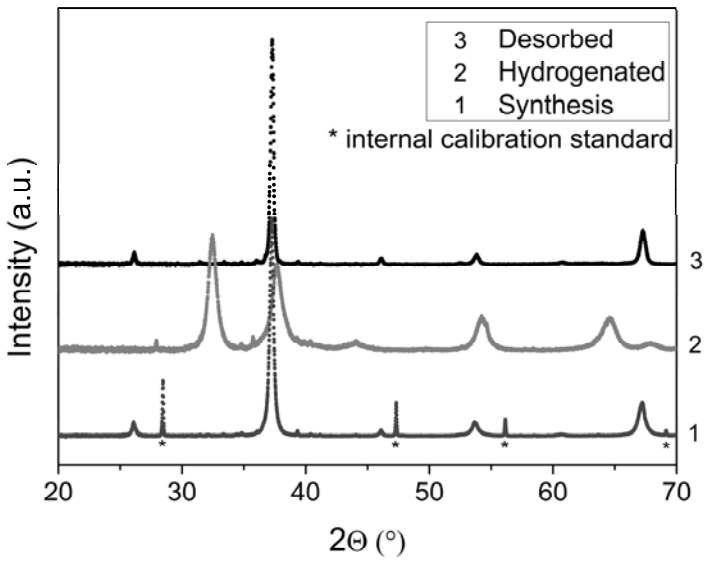

Figure 6.8. XRD of $ScAl_{0.8}Mg_{0.2}$ after synthesis, hydrogenation and desorption. Si is used as internal calibration standard.

By comparing the desorption temperature (T_m) observed for hydrogenated $ScAl_{0.8}Mg_{0.2}$ (~500 °C) with the reported desorption temperature (960 °C) [53] it was observed that there was a significant destabilisation of ScH_2 due to the presence of magnesium and aluminium. These results are in good agreement with the theoretical calculations, discussed below.

From DFT calculations it was concluded that the CsCl-type structure was the most stable structure for the mother compound, as compared with the random W-type (body-centred cubic) and cubic close-packed structures. It was also found that during hydrogen absorption there was a phase separation where the hydrogen atoms preferably occupied positions coordinated by scandium atoms. According to the calculations should the phase separated sample be stable at atmospheric pressure up to ~330 °C (~600 K), a value in good agreement with the experiments. The somewhat higher temperature observed experimentally could be due to kinetic barriers or the approximations used in the theoretical study.

6.2.2 $Sc(Al_{1-x}Mg_x)$, $x \leq 0.20$

Solid solutions of magnesium in ScAl were investigated in Paper VIII to evaluate the magnesium influence on the hydrogen storage properties of $Sc(Al_{1-x}Mg_x)$. Samples ranging from x = 0 - 0.20 were investigated. It was shown that all samples crystallize in the CsCl-type structure. The unit cell parameter of the samples followed Vegard's law, as shown in figure 6.9.

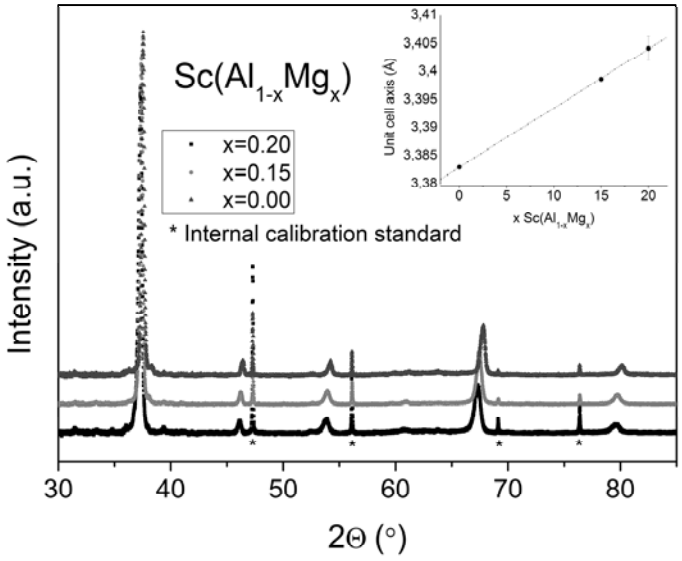

Figure 6.9. XRD pattern of $Sc(Al_{1-x}Mg_x)$, $x \leq 0.20$. From the top: x = 0, 0.15, 0.20. Silicon is used as internal calibration standard. The inset shows the unit cell axis as a function of magnesium content.

TDS measurements showed that the small peak (at ~365 °C) was only present for x > 0.15 (Figure 6.10). One possible explanation is that the maximum solid solution of magnesium in aluminium has been determined to 18.6 at.% [54]. The additional magnesium, for the x = 0.20 sample might form X-ray amorphous MgH_2. Both T_m and the activation energy fitted very well with the results of Han *et al.* on the desorption of magnesium hydride[55]: the small peak for x = 0.20 was 139 kJ/mol and the reported value was 142 kJ/mol.

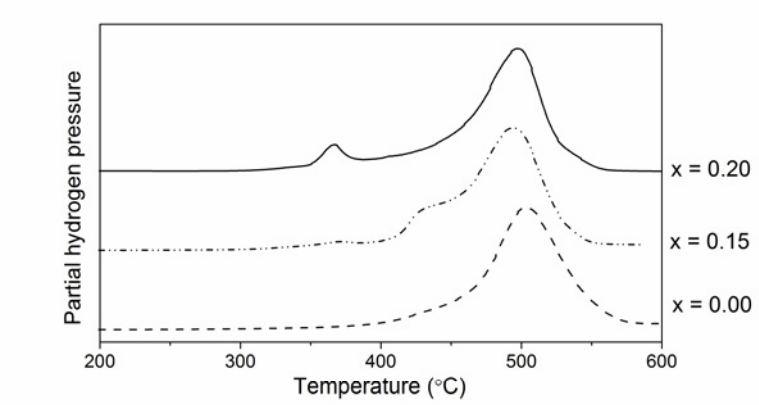

Figure 6.10. Thermal desorption spectra of hydrogenated $Sc(Al_{1-x}Mg_x)$ for x = 0, 0.15 and 0.20, recorded for the first absorption/desorption cycle. The heating rate was 5 °C/min.

Five absorption/desorption cycles were performed on $Sc(Al_{1-x}Mg_x)$ for x = 0 where the hydrogenated sample was first desorbed in UHV and then rehydrogenated at 70kPa and 420 °C. After five cycles, TDS was performed for the sixth desorption. The thermal desorption spectra for the first and sixth desorption are shown in Figure 6.11. The temperature of maximum desorption was increased about 15 °C by cycling the material. Small amounts of $ScAl_2$ and Sc_2O_3 were formed during cycling, seen from XRD. The presence of small amounts of oxygen could not be avoided in the experimental conditions.

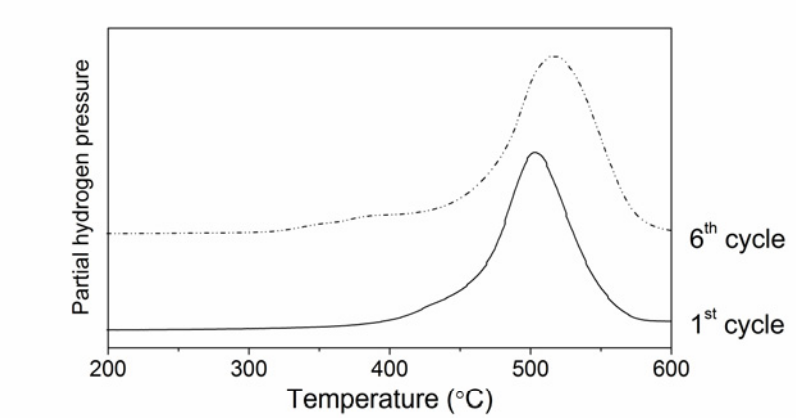

Figure 6.11. Thermal desorption spectra of $Sc(Al_{1-x}Mg_x)$ for x = 0.0, recorded during the first and sixth desorption cycle.

SEM investigations showed no change in particle size during cycling (Figure 6.12). The particle size was unaffected by cycling the material. From EDS, the overall composition of the samples could be confirmed. The small grains of ScH_2 and Al(Mg) could not be observed, only from a high-resolution image an indication of the grains could be seen, Figure 6.13. The grain size of ScH_2 and Al(Mg) from SEM was estimated to 10-20 nm.

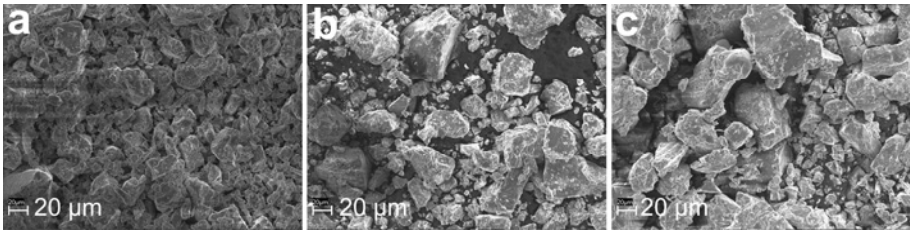

Figure 6.12. a, SEM images of the hydrogenated sample ($Sc(Al_{1-x}Mg_x)$, x = 0.20). b, Desorbed sample (x = 0.20). c, Hydrogenated sample after six cycles (x = 0.0). Magnification 1000 x.

The fact that the particle size did not change during hydrogen loading and unloading was unanticipated as the HDDR behaviour seen from XRD commonly reduces the particle size of the material[52]. The constancy of the particle size could explain that there was no lowering of the maximum desorption temperature from cycling, which is commonly attributed to a reduced particle size.

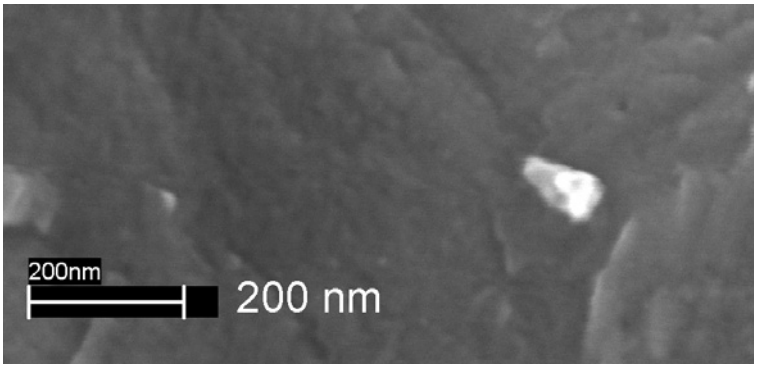

Figure 6.13. High-resolution SEM image of the hydrogenated sample ($Sc(Al_{1-x}Mg_x)$, x = 0.20). Magnification 380 kx.

6.3 Summary of the Sc-Mg-based alloys

A summary of the hydrogen absorption and desorption behaviour of all the investigated compounds is listed in Table 2. According to the results presented in Paper VI-VIII the hydrogen interactions with Sc-Mg-based alloys were not as strong as in the Y-Mg-based alloys. Sc_2MgGa_2 did not react with hydrogen at all at the investigated temperature and hydrogen pressure range. $Sc(Al_{1-x}Mg_x)$ decomposed during hydrogen absorption, but the reaction was fully reversible. All investigated $Sc(Al_{1-x}Mg_x)$ samples exhibited the HDDR behaviour, a property not observed before in neither Sc-Al- or Sc-Mg-based alloys. Furthermore, the $Sc(Al_{1-x}Mg_x)$ alloys were very stable towards air oxidation, the samples showed no significant degradation after storing in air for more than three months.

The $Sc(Al_{1-x}Mg_x)$ alloys were very stable and safe to handle which is of importance for practical applications. It is expected that further research of these alloys, possibly with other alloying elements, will lead to new modifications that release hydrogen at lower temperatures. Therefore, there is a perspective for future applications of these scandium based materials. These results may also inspire to design other new classes of materials for hydrogen storage.

Table 2. *Summary of the hydrogen absorption/desorption behavior of the investigated compounds.*

Compound	**Hydrides**	**Reversibility**	**Desorption product**
$Mg_{24}Y_5$	MgH_2 & YH_3	Partial	YH_2 & Mg
YMgGa	YH_3 & MgGa	Partial	YMgGa, YGa_2, Mg & YH_2
$Mg_{12}YZn$	Decomposes	-	-
$Mg_3Y_2Zn_3$	YH_3, MgH_2 & $MgZn_2$	Partial	Mg_3YZn_6, MgH_2 & YH_2
Sc_2MgGa_2	No absorption	-	-
$Sc(Al_{1-x}Mg_x)$	ScH_2 & Al(Mg)	Complete	$Sc(Al_{1-x}Mg_x)$

7. Concluding remarks

7.1 Parameters influencing hydrogen storage properties

In order to obtain a hydrogen storage material with stable cycling performance and with a high reversible storage capacity, there are a number of parameters that are crucial to understand. The crystal structure is a key parameter in order to understand the different reactions taking place during absorption and desorption. The hydrogen occupied sites in a crystal cannot be closer than 2 Å[56], and hydrogen usually prefers a site with a certain size. Thus, there can be a limitation caused by the crystal structure even though the elements are expected to absorb hydrogen. By knowing the crystal structure of the alloys and their hydrides it is usually easier to explain the experimental behaviour of the system.

The microstructure is a parameter that influences the kinetic properties. It has been shown that grain size is a key parameter to gain rapid absorption and desorption. In both the Y-Mg and Y-Mg-Ga systems it is evident that the smaller grains achieved by cycling the material improves the desorption kinetics, the importance of grain size on desorption temperature is a known phenomena[57].

The thermodynamic properties are essential for the storage properties. As shown for the Y-Mg-Ga system, it was possible to lower the desorption temperature of yttrium by ~400 °C by introducing gallium. In this system, gallium reacts with yttrium and forms YGa_2. The stability of this phase is higher than for pure yttrium and thus it will decrease the energy needed to desorb hydrogen from yttrium. The same type of behaviour was observed in the Sc-Al-Mg system. This type of thermodynamic destabilisation is a promising instrument for tuning the thermodynamic properties.

By forming a metal hydride that interacts in a good way with hydrogen, both regarding thermodynamics and kinetics, and that can store large amounts of hydrogen there could be a future for metal hydrides in vehicular applications.

7.2 Synthesis of new materials

To summarize all knowledge about metal-hydrogen systems it might be possible to draw some conclusions about the future of hydrogen storage. None

of the compounds that are known today fulfil all the goals that are required for a storage material for hydrogen powered vehicles. There has to be a continued search for new materials that can store large amounts of hydrogen in a safe and practical way. The aim of this thesis has been to gain fundamental knowledge about metallic magnesium compounds and to study the hydrogen absorption and desorption properties. The $Sc(Al_{1-x}Mg_x)$ compounds showed reactions with hydrogen which to some extends were unexpected and promising in order to find new functional materials for hydrogen storage.

Acknowledgements

First of all I would like to thank my supervisor Professor Yvonne Andersson for all your support through this period. Thank you for generously sharing your extensive knowledge and for always encouraging me. You have truly been a great supervisor! Thanks also to my co-supervisor Björgvin Hjörvarsson for showing me the strange and exiting world of physics.

I would also like to thank Dr. Claudia Zlotéa for all your help and for being such a good friend at numerous conferences and meetings. I look forward to continue working with you.

Thanks to all the co-authors to the papers included in this thesis, your help has been invaluable in making this thesis. Thanks also to Professor Jan-Otto Carlsson for keeping such excellent research facilities at our disposal at the Ångström Laboratory.

Financial support from The Royal Swedish Academy of Sciences and Helge Ax:son Johnsons stiftelse is gratefully acknowledged.

Thanks to the technical staff, Anders Lund, Peter Lundström, Hendrik Eriksson and Janne Bohlin for always keeping the equipment in such a good shape. The administrative staff, Gunilla Lindh, Eva Larsson and Katarina Israelsson are acknowledged for always being helpful and keeping the department in order.

Thanks to Professor Torjörn Gustafsson and Håkan Rundlöf for all your help with the diffractometers.

I would also like to thank Dr. Mikael Ottosson for all your skilful help in the basement and with powder diffraction.

I am grateful to all colleagues and friends, past and present, at the Department of Materials Chemistry for making it such a good place to work.

Thanks to Erik[2], Erika and Anna for your support and good company during this last “summer of writing”, good luck to you all!

A special thanks to my dear friends from the department, Anton, Hanna and Daniel for all the laughs and for believing in me!

Ett stort tack till alla mina vänner som har påmint mig om livet utanför jobbet, nu kommer jag att ha tid för er igen!

Tack till min familj för att ni alltid har trott på mig och för att ni alltid finns där och stöttar när det känns tungt! Tack även till Saras familj för att ni tagit emot mig med öppna armar, trots att jag är en ”biologisk analfabet”.

Tack underbara Sara och Ester för att ni gör livet värt att leva, jag älskar er så!

/Martin Sahlberg

Summary in Swedish

Ren energi och energimaterial är ett område inom vetenskapen som har fått otroligt mycket uppmärksamhet de senaste åren. Detta har naturligtvis att göra med den globala uppvärmningen och de stora utsläppen av växthusgaser. Den kemiska förening som anses vara boven i dramat är koldioxid, CO_2. Koldioxiden i atmosfären absorberar värmestrålning som jorden sänder ut och skickar tillbaka den mot jorden, vilket gör att jorden värms upp.

En del av all koldioxid som finns i luften kommer från fordonsutsläpp. När kolväten (bensin, olja etc.) förbränns med syret i luften bildas koldioxid och vatten enligt formeln nedan:

$$C_xH_y + O_2 \rightarrow CO_2 + H_2O + \text{energi}$$

Den energi som frigörs kan användas för att till exempel driva en bil. Detta är den princip som används i de absolut flesta fordon idag. Om man istället skulle använda väte som bränsle skulle reaktionen se annorlunda ut:

$$H_2 + \tfrac{1}{2}O_2 \rightarrow H_2O + \text{energi}$$

När väte reagerar med syre frigörs också energi, ungefär tre gånger så mycket per kilo bränsle, och biprodukten är då enbart vatten.

Det finns två sätt att använda energin i väte, antingen genom att förbränna vätet och få ut energi i form av värme, eller att låta det reagera med syre i en bränslecell och få ut energi som elektricitet. Om man jämför energieffektiviteten i en vätedriven bränslecell och en vanlig bensindriven förbränningsmotor så är det dessutom en trefaldigad effektivitetsökning om man använder väte istället för bensin, dvs. väte är ett både effektivare och renare bränsle.

Ett av de stora problemen med att använda väte som energibärare istället för kolväten är att väte är svårt att lagra. Vid normalt tryck och temperatur är väte en gas, viket leder till svårigheter om man vill lagra stora mängder väte i en liten volym. Det finns tre huvudsakliga sätt att lagra väte: i högtryckstankar, i vätskeform vid -250 °C och kemiskt bundet i metallhydrider. De två första sätten är de sätt som används idag, båda fungerar relativt bra men är inte tillräckligt effektiva för att bli en permanent lösning. Inget av sätten kan

uppfylla kraven på tankens storlek och vikt för att kunna användas i vanliga fordon.

Metallhydrider uppstår när väte reagerar med en metall eller legering och bildar en stabil förening. Dessa föreningar har ofta en hög energitäthet men medför istället problem med att få in och ut vätet vid rimliga temperaturer och tryck.

Målet med forskningen som presenteras i denna avhandling är att finna nya legeringar som kan lagra stora mängder väte, och som dessutom har egenskaper som gör materialet praktiskt användbart, inte minst viktsmässigt.

Magnesium är en metall som reagerar med väte och bildar magnesiumhydrid, MgH_2. Denna förening innehåller 7,6 vikts% väte, vilket gör den till en väldigt intressant kandidat för vätelagring. Ett av de stora problemen med magnesiumhydrid är dock att det krävs höga temperaturer för att få in och ut vätet ur magnesium. Detta beror på den dåliga rörligheten av väte i magnesiumhydrid: så fort ett korn av magnesium börjar reagera med väte bildas ett ytlager av magnesiumhydrid som hindrar mer väte att gå in och därför gör det svårt att utnyttja hela kapaciteten hos materialet.

I den här avhandlingen har jag studerat två sätt att förbättra lagringsegenskaperna hos magnesiumbaserade legeringar: Det ena är att tillverka väldigt små magnesiumstrukturer och på så sätt minska de avstånd som väteatomerna måste tillryggalägga inuti legeringen. Det andra är att legera magnesium med andra metaller och på så sätt ändra egenskaperna hos materialet. Jag har huvudsakligen studerat legeringar mellan magnesium och yttrium samt magnesium och skandium. Både yttrium och skandium bildar hydrider och har tidigare visat möjligheter att förbättra lagringsegenskaperna hos legeringar med magnesium.

Ett av de studerade materialen som uppvisat väldigt goda egenskaper är en ny legering av skandium, aluminium och magnesium: $ScAl_{0.8}Mg_{0.2}$. Detta material tar upp väte genom att sönderdelas till skandiumhydrid (ScH_2) och aluminium med magnesium i fast lösning (Al(Mg)) enligt formeln nedan:

$$ScAl_{0.8}Mg_{0.2} + H_2 \leftrightarrow ScH_2 + Al(Mg)$$

Reaktionen är fullständigt reversibel (kan gå åt endera hållet) och materialet kan lagra 2,7 vikts% väte. I figur 1 nedan visas en studie av hur materialet tar upp väte och sönderfaller till ScH_2 och Al(Mg). Studien är utförd med röntgendiffraktion vid synkrotronanläggningen MAX-lab i Lund. Väteabsorptionen i materialet går väldigt snabbt, det tar endast ~3 minuter från det att materialet börjar ta upp väte tills reaktionen är fullständig. Detta är en väldigt bra egenskap hos ett material om man vill kunna använda det praktiskt.

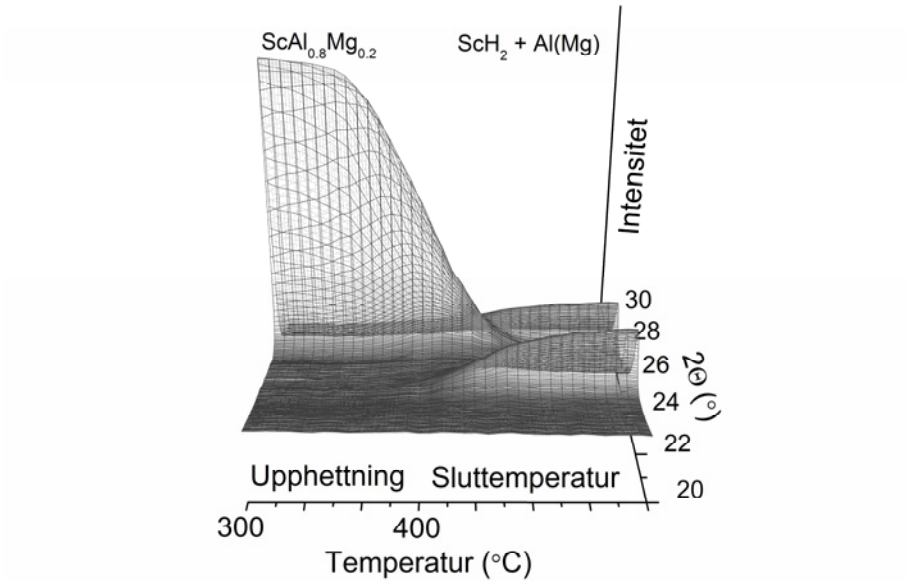

Figur 1. Studie av reaktionen då $ScAl_{0.8}Mg_{0.2}$ absorberar väte och sönderfaller till ScH_2 och Al(Mg).

Alla mina studier i denna avhandling visar att väteabsorptionen i metaller är komplex och att varje material måste optimeras enligt sina unika egenskaper. Ett material som ska kunna användas för att lagra väte i fordonstillämpningar måste ha mycket goda egenskaper både vad gäller lagringskapacitet och reaktionshastighet. Det behöver även vara billigt, vilket tyvärr inte skandium är. Mina resultat visar att det går att finna nya och lätta väteabsorberande material och att deras lagringsegenskaper går att optimera.

References

[1] European Commission. EUR 20719 EN - Hydrogen Energy and Fuel Cells - A vision of our future, **2003**.
[2] Chalk, S.G.; Miller, J.F. *Journal of Power Sources* **2006**, *159*, 73.
[3] Lovins, A.B. Twenty Hydrogen Myths; Rocky Mountain Institute: Snowmass, **2003**.
[4] Holladay, J.D.; Hu, J.; King, D.L.; Wang, Y. *Catalysis Today* **2009**, *139*, 244.
[5] Tributsch, H. *International Journal of Hydrogen Energy* **2008**, *33*, 5911.
[6] Ghirardi, M.L.; Zhang, L.; Lee, J.W.; Flynn, T.; Seibert, M.; Greenbaum, E.; Melis, A. *Trends in Biotechnology* **2000**, *18*, 506.
[7] Mori, D.; Hirose, K. *International Journal of Hydrogen Energy* **2009**, *34*, 4569.
[8] Graham, T. *Journal of the Chemical Society* **1867**, *20*, 235.
[9] Van Vucht, J.H.N.; Kuijpers, F.A.; Bruning, H.C.A.M. *Philips Research Reports* **1970**, *25*, 133.
[10] Willems, J.J.G.; Buschow, K.H.J. *Journal of the Less-Common Metals* **1987**, *129*, 13.
[11] Sandrock, G. *Journal of Alloys and Compounds* **1999**, *293-295*, 877.
[12] Reilly, J.J.; Wiswall, R.H. *Inorganic Chemistry* **1968**, *7*, 2254.
[13] Noreus, D. *Zeitschrift für Physikalische Chemie* **1989**, *163*, 575.
[14] Dymova, T.N.; Eliseeva, N.G.; Bakum, S.I.; Dergachev, Y.M. *Doklady Akademii Nauk SSSR* **1974**, *215*, 1369.
[15] Bogdanovic, B.; Schwickardi, M. *Journal of Alloys and Compounds* **1997**, *253-254*, 1.
[16] Bogdanovic, B.; Felderhoff, M.; Streukens, G. *Journal of the Serbian Chemical Society* **2009**, *74*, 183.
[17] Ellinger, F.H.; Holley, C.E.; McInteer, B.B.; Pavone, D.; Potter, R.M.; Staritzky, E.; Zachariasen, W.H. *Journal of the American Chemical Society* **1955**, *77*, 2647.
[18] Stampfer, J.F.; Holley, C.E.; Suttle, J.F. *Journal of the American Chemical Society* **1960**, *82*, 3504.
[19] Selvam, P.; Viswanathan, B.; Swamy, C.S.; Srinivasan, V. *International Journal of Hydrogen Energy* **1986**, *11*, 169.
[20] Sakintuna, B.; Lamari-Darkrim, F.; Hirscher, M. *International Journal of Hydrogen Energy* **2007**, *32*, 1121.
[21] Reilly, J.J.; Wiswall, R.H. *Inorganic Chemistry* **1967**, *6*, 2220.
[22] Buchner, H.; Bernauer, O.; Straub, W. *Hydrogen Energy Systems, Proceedings of the 2nd World Hydrogen Energy Conference in Zürich, 21-24 August 1978* (Edited by Veziroglu T.N. and Seifritz W. Pergamon Press, New York) **1978**, 1677.

[23] Douglas, D. *Hydrides for Energy Storage, Proceedings of an International Symposium held in Geilo, Norway, 14-19 August 1977* (Edited by Andresen A.F. and Maeland A.J. Pergamon press) **1978**, 151.
[24] Chacon, C.; Johansson, E.; Hjörvarsson, B.; Zlotea, C.; Andersson, Y. *Journal of Applied Physics* **2005**, *97*, 104903/1.
[25] Goto, Y.; Kamegawa, A.; Takamura, H.; Okada, M. *Materials Transactions* **2002**, *43*, 2717.
[26] Ogawa, K.; Aoki, H.; Kobayashi, T. *Journal of the Less-Common Metals* **1982**, *88*, 283.
[27] Latroche, M.; Kalisvaart, P.; Notten, P.H.L. *Journal of Solid State Chemistry* **2006**, *179*, 3024.
[28] Kalisvaart, W.P.; Latroche, M.; Cuevas, F.; Notten, P.H.L. *Journal of Solid State Chemistry* **2008**, *181*, 1141.
[29] Cerenius, Y.; Stahl, K.; Svensson, L.A.; Ursby, T.; Oskarsson, A.; Albertsson, J.; Liljas, A. *Journal of Synchrotron Radiation* **2000**, *7*, 203.
[30] Bruker AXS Inc., Madison, Wisconsin, USA **2001**.
[31] Sheldrick, G.M. *Acta Crystallographica* **2008**, *A64*, 112.
[32] Rietveld, H.M. *Journal of Applied Crystallography* **1969**, *2*, 65.
[33] Rodríguez-Carvajal, J. *FullProf.2k computer program, version 2.90* **2004**.
[34] Flanagan, T.B. *Hydrides for Energy Storage, Proceedings of an International Symposium held in Geilo, Norway, 14-19 August 1977* (Edited by Andresen A.F. and Maeland A.J. Pergamon press) **1978**, 43.
[35] Kissinger, H.E. *Analytical Chemistry* **1957**, *29*, 1702.
[36] Von Zeppelin, F.; Haluska, M.; Hirscher, M. *Thermochimica Acta* **2003**, *404*, 251.
[37] Hohenberg, P.; Kohn, W. *Physical review* **1964**, *136*, B864.
[38] Perdew, J.P.; Burke, K.; Ernzerhof, M. *Physical Review Letters* **1996**, *77*, 3865.
[39] Bonhomme, F.; Yvon, K. *Journal of Alloys and Compounds* **1996**, *232*, 271.
[40] Smith, J.F.; Bailey, D.M.; Novotny, D.B.; Davison, J.E. *Acta Metallurgica* **1965**, *13*, 889.
[41] Zlotea, C.; Lu, J.; Andersson, Y. *Journal of Alloys and Compounds* **2006**, *426*, 357.
[42] Yartys, V.A.; Gutfleisch, O.; Panasyuk, V.V.; Harris, I.R. *Journal of Alloys and Compounds* **1997**, *253-254*, 128.
[43] Zlotea, C.; Andersson, Y. *Acta Materialia* **2006**, *54*, 5559.
[44] Kraft, R.; Valldor, M.; Pottgen, R. *Zeitschrift für Naturforschung B: Journal of Chemical Sciences* **2003**, *58*, 827.
[45] Yoshida, M.; Akiba, E.; Shimojo, Y.; Morii, Y.; Izumi, F. *Journal of Alloys and Compounds* **1995**, *231*, 755.
[46] Rundqvist, S.; Jellinek, F. *Acta Chemica Scandinavica* **1959**, *13*, 425.
[47] Yannopoulos, L.N.; Edwards, R.K.; Wahlbeck, P.G. *Journal of Physical Chemistry* **1965**, *69*, 2510.
[48] Babu, R.; Nagarajan, K.; Venugopal, V. *Journal of Alloys and Compounds* **2000**, *311*, 200.
[49] Rieger, W.; Nowotny, H.; Benesovsky, F. *Monatshefte für Chemie* **1964**, *95*, 1502.
[50] Zachariasen, W.H. *Acta Crystallographica* **1949**, *2*, 94.
[51] Grobner, J.; Schmid-Fetzer, R.; Pisch, A.; Cacciamani, G.; Riani, P.; Parodi, N.; Borzone, G.; Saccone, A.; Ferro, R. *Zeitschrift für Metallkunde* **1999**, *90*, 872.
[52] Harris, I.R.; McGuiness, P.J. *Journal of the Less-Common Metals* **1991**, 172-*174*, 1273.

[53] Aleksanyan, A.G.; Dolukhanyan, S.K.; Shekhtman, V.S.; Harutyunyan, K.S.; Abrahamyan, K.A.; Mnatsakanyan, N.L. *Journal of Alloys and Compounds* **2003**, *356-357*, 562.
[54] Murray, J.L. *Bulletin of Alloy Phase Diagrams* **1982**, *3*, 60.
[55] Han, J.S.; Pezat, M.; Lee, J.Y. *Journal of the Less-Common Metals* **1987**, *130*, 395.
[56] Switendick, A.C. *Zeitschrift für Physikalische Chemie* **1979**, *117*, 89.
[57] Varin, R.A.; Czujko, T.; Wronski, Z. *Nanotechnology* **2006**, *17*, 3856.

Acta Universitatis Upsaliensis

Digital Comprehensive Summaries of Uppsala Dissertations from the Faculty of Science and Technology 666

Editor: The Dean of the Faculty of Science and Technology

A doctoral dissertation from the Faculty of Science and Technology, Uppsala University, is usually a summary of a number of papers. A few copies of the complete dissertation are kept at major Swedish research libraries, while the summary alone is distributed internationally through the series Digital Comprehensive Summaries of Uppsala Dissertations from the Faculty of Science and Technology. (Prior to January, 2005, the series was published under the title "Comprehensive Summaries of Uppsala Dissertations from the Faculty of Science and Technology".)

Distribution: publications.uu.se
urn:nbn:se:uu:diva-107380

ACTA
UNIVERSITATIS
UPSALIENSIS
UPPSALA
2009